Nuclear Engineering and Technology 51 (2019) 95–103

Contents lists available at ScienceDirect

Nuclear Engineering and Technology

journal homepage: www.elsevier.com/locate/net

Original Article

Stratified steam explosion energetics

HangJin Jo*, Jun Wang, Michael Corradini

Department of Engineering Physics, University of Wisconsin, Madison, WI, 53706, USA

ARTICLE INFO

Article history:
Received 3 May 2018
Received in revised form
19 July 2018
Accepted 24 August 2018
Available online 7 September 2018

Keywords:
Steam explosion
Stratified configuration
Pool configuration
Fuel-coolant mixing

ABSTRACT

Vapor explosions can be classified in terms of modes of contact between the hot molten fuel and the coolant, since different contact modes may affect fuel-coolant mixing and subsequent vapor explosion energetics. It is generally accepted that most vapor explosion phenomena fall into three different modes of contact; fuel pouring into coolant, coolant injection into fuel and stratified fuel-coolant layers. In this study, we review previous stratified steam explosion experiments as well as recent experiments performed at the KTH in Sweden. While experiments with prototypic reactor materials are minimal, we do note that generally the energetics is limited for the stratified mode of contact. When the fuel mass involved in a steam explosion in a stratified geometry is compared to a pool geometry based on geometrical aspects, one can conclude that there is a very limited set of conditions (when melt jet diameter is small) under which a steam explosion is more energetic in a stratified geometry. However, under these limited conditions the absolute energetic explosion output would still be small because the total fuel mass involved would be limited.

1. Introduction

A severe accident can occur given a prolonged absence of normal cooling to the reactor core as well as failure of emergency core cooling systems. Without operator actions to provide alternate water cooling, the core decay heat would eventually cause the core materials to melt. These materials could slump into the lower plenum leading to reactor pressure vessel failure and melt relocation to the reactor cavity. Depending on specific reactor designs, when molten core materials move to the lower plenum of the reactor vessel or the reactor cavity, the molten core materials could interact with residual coolant water; so-called fuel-coolant interaction (FCI). In a FCI rapid boiling can occur caused by fuel fragmentation and heat transfer from molten core materials ('corium') to the water coolant. If the rate of fuel fragmentation and heat transfer is rapid enough, this can lead to local dynamic shock pressurization and propagation; i.e., a steam explosion that can threaten structural integrity of containment components.

Steam explosions can be classified in terms of modes of contact between the hot fuel and cold liquid coolant, since different contact modes can affect fuel-coolant mixing and thereby affect vapor explosion energetics. The configuration depends on the fuel entry conditions, coolant conditions and geometrical arrangement. In the case of corium release into a cavity with remaining water, a pouring mode of contact is expected. Steam explosions have been investigated extensively in this contact mode, a likely geometry in postulated nuclear accidents as well as for actual accidents in non-nuclear industries [1–4]. In this geometry, the corium jet pours into the water, and can break up into fragments due to relative velocity induced instabilities [5–7]. As the corium mixes with water in film boiling, local vapor film collapse may occur and trigger rapid fuel fragmentation. This will increase the heat transfer area causing significant local pressurization. This generates shock wave propagation throughout the already mixed corium in water pool, thereby causing an energetic explosion.

A different fuel-coolant contact mode occurs in a stratified geometry. In contrast to the pouring mode, the stratified explosion considers that the molten corium and coolant are completely separated by a stable vapor film [8]. Such a contact mode could occur in a situation where water refloods a cavity region with corium already present or when the water level is low and the corium pours accumulates on the cavity floor without triggering during its pour into the shallow water pool. In contrast to the pouring mode of steam explosions, fuel-coolant mixing is not considered in the stratified geometry. However, fluid instabilities during boiling can cause vapor film collapse, and local mixing. In this configuration, the explosion is due to propagation of local vapor film collapse along the interface between the fuel and coolant

* Corresponding author.
E-mail address: jo23@wisc.edu (H. Jo).

https://doi.org/10.1016/j.net.2018.08.019

layers.

In this work we first review previous stratified steam explosion experiments including recent simulant experiments conducted at KTH [12–14]. Next we compare a theoretical fuel fragmentation explosion model between the pouring mode of contact and the stratified mode of contact [8]. This comparison allows us to examine under what conditions the stratified mode explosion energetics can exceed the pouring mode explosion energetics. These analyses can help inform us as to the likely range of stratified steam explosion energetics.

2. Review of stratified steam explosion experiments

2.1. Previous stratified steam explosion experiments

In this section, we review previous stratified steam explosion experiments conducted at Sandia National Laboratories (SNL), the Joint Research Center at Ispra (JRC), Argonne National Laboratory (ANL and UW-Madison). This brief review of these past experiments suggests that prototypic experimental data are quite limited, but simulant experiments for a stratified contact mode can provide additional insight to this limited database.

The SNL ACM (Alternative Contact Mode) experiments consisted of two experiments for a stratified contact mode vapor explosion [9]. In these two tests, water was gently poured into a graphite crucible (a few inches in diameter) on top of a high temperature melt (a mixture of alumina and iron) generated by the thermite reaction. The explosion occurred spontaneously in ACM-1, having a short delay time; i.e., the time between completion of the thermite reaction that produced the melt and the water pour onto the melt. In the ACM-2 test, the delay time was increased and no spontaneous explosion occurred, presumably due to the formation of a solid crust on top of the melt before water addition. These tests had no instrumentation to quantify the conversion ratio to mechanical work from the melt thermal energy.

A molten melt spreading experiment into a shallow water layer was performed at JRC-Ispra (FARO L-26S) [10]. In this test a stainless steel plate forming an angular sector of 17° was used as the representative basemat surface. This spreading plate was covered with a shallow water layer 10 mm high. The test objective was to deliver a corium (128 kg of 80w% UO_2 - 20w% ZrO_2) melt pour and observe spreading behavior at a moderate flow rate (about 2 l/s) into water. With a melt temperature of 3000 K similar other FARO tests where an FCI occurred, there was no steam explosion observed. In the test report, researchers focused on describing the spreading of the melt with temperature of the basemat plate, melt spreading distance, melt height, and debris morphology. This was part of a larger program of melt spreading into a dry cavity.

Argonne National Lab reported four series of experiments with different techniques to quantify stratified steam explosions [11]. In their first stratified steam explosion series of tests, 85–95 °C water was gently poured onto 600–700 °C molten tin prepared in a long (1 m) and narrow chamber (50 mm wide x 90 mm deep), forming a 30 mm molten tin layer. Experimental results showed that weak spontaneous explosions occurred over wide time ranges. In the second and third series of experiments a vertical chamber (0.3 m long × 50 mm wide × 50 mm deep) was built, allowing two liquid columns (Freon-22 as the coolant and water as the fuel) to be poured into the chamber respectively. All tests failed to produce the reproducible vertically stratified explosions due to the premature mild interactions. In the fourth test series with the same vertical chamber, Freon-22 (coolant) and water (fuel) were poured in the chamber and were separated by 0.25 mm mylar diaphragm, and by rapidly removing the mylar diaphragm the stratified geometry was formed. The explosive interaction was triggered from the bottom of the chamber due to a trigger pulse and propagated vertically upward. The steam explosions were observed at most tests, and a peak pressure and shock propagation speed were measured, 1 MPa and 150 m/s respectively. No measurements were made to quantify the conversion ratio to mechanical work from the melt thermal energy.

Bang and Corradini [8] conducted stratified steam explosion experiments with different liquid pairs (water/liquid nitrogen and water/Freon-12) in test sections of two different sizes; a small scale (25 mm wide × 0.2 m long and 0.65 m high for water/LN_2 tests and 1.26 m high for the water/R12 tests) and a large scale (64 mm wide × 0.5 m long × 1.5 m high). The interactions were either triggered by an external trigger or allowed to occur spontaneously depending on the liquid pair and initial conditions. The major experimental variables were initial water temperature, liquid layer depths, and magnitude of the external trigger pressure. The experiments were designed to determine the fuel-coolant interactions depths of liquid-liquid mixing during the explosion propagation and the dependence of these interactions depths on the liquid layer depths were observed; i.e., these interaction depths were found to be small (<1 cm). Based on the hypothesis that this liquid-liquid mixing process was controlled by Rayleigh-Taylor instability phenomena, a model for the depth of intermixing was proposed. This model allows one to estimate the mixing dynamics of stratified steam explosion based on key geometric parameters, the length of the liquid layer interface and the depth of the top liquid.

2.2. Simulant steam explosion experiments by KTH

The Royal Institute of Technology in Sweden (KTH) performed a series of stratified steam explosion tests with two different facilities recently [12–14]; PULiMS and SES. PULiMS and SES facilities employ the same melt preparation technique consisting of 45 kW induction furnace with a SiC crucible for melt preparation and melt delivery via a funnel. The melt was poured into a spreading chamber containing a shallow water layer. Each chamber had different dimensions (PULiMS: 2 m wide × 1 m long × 1 m high, SES: 1 wide × 1 m long × 0.8 m high). Once the melt has reached a prescribed temperature it was released from the melt generator through the delivery funnel into the chamber. The initial water depth was fixed as 0.2 m in all PULiMS and SES tests. The molten jet pour diameter was fixed at PULiMS as 20 mm while SES had 20 and 30 mm jet diameters. Six tests were conducted in PULiMS and three tests resulted in steam explosions. Only the last test (E6-PULiMS) measured the explosion impulse (integrated force-time curve over the chamber base) because force measurements were not used in the first five tests. The PULiMS facility was initially built to examine molten melt spreading phenomena like the FARO tests. KTH researchers estimated the impulse for the previous five tests using measured residual plastic deformation (deflection) of the bottom spreading plate. This technique was benchmarked by comparing the estimated impulse for E6 by this approach with the measured impulse at E6. The estimated impulse for E6 ranged from 2 to 15% deviation from PULiMS E6 data based on deformation analysis. In the SES experiments, two out of three tests resulted in a steam explosion, with the explosion impulse computed from force measurements on the chamber base. Thus, KTH researchers report the steam explosion kinetic energy and its efficiency using the force measurements to compute the explosion impulse and its kinetic energy.

In KTH's conference publications, the steam explosion efficiency was defined as

$$\varepsilon = E_{released}/E_t \quad (1)$$

where E_{released} denotes total released energy and E_{t} indicates thermal energy of the melt poured into the test chamber, respectively. In one of their early publications, they defined E_{released} as the summation of kinetic energy, energy dissipated during bottom plate deformation, and support frame deformation [13]. However, the dissipated energies by the bottom plate and the support frame deformation were insignificant compared to the computed kinetic energy. After this early publication, KTH only used the kinetic energy to represent E_{released}. The kinetic energy was estimated as

$$E_k = I^2/2m_w \quad (2)$$

where I is impulse from the interaction (integrated force with respect to time), and m_{w} is mass of accelerated water. Because the exact mass of water accelerated during the explosion was not measurable, they reported their results with different masses of water corresponding to varying diameters of accelerated water column ranging from 0.4 to 1.0 m times the initial water depth. The diameter of 0.4 m corresponds to melt spreading area detected by TCs and was chosen as the most plausible interaction area for PULiMS E6. The diameter of 1.0 m is the width of the spreading plate and thus is a maximum possible value, which gives lowest possible efficiency. As we have reviewed the reported data, this is the largest uncertainty in the explosion energetics analysis.

As noted, KTH researchers assumed the mass of accelerated water amount by variation of the assumed diameter of water column. However, they did not clearly document the height of the water column. For the height used for the accelerated water column, we back-calculated from the reported water mass, based on the assumed surface area given in their papers and water density. The height used for the water column was ranged from 0.166 to 0.168 m water height for PULiMS E6, which does not correspond to the reported initial water level (0.2 m). If we use the initial water level (0.2 m) for the calculation instead of 0.166–0.168 m, their reported explosion kinetic energy and efficiency will be 88% of the reported values; a second-order effect but notable. According to the back-calculation for the height used for the water column, they changed the height of water level for different cases (0.13–0.21 m for SES cases), but they did not clarify how the height of water column was determined. We will discuss alternative approaches for determination of the accelerated water mass, m_{w}.

The term, m_{w}, corresponds to the mass of water accelerated by the explosion impulse, as measured in the experiments. The analysis assumes a one-dimensional expansion and in reality the explosion expansion has multi-dimensional aspects. In this regard, one may consider an alternative approach for estimating m_{w}. Consider the explosion impulse propagation as described by the water-steam sound speed and the explosion duration. In PULiMS E6, KHT noted that m_{w} is the water mass that was accelerated for an impulse duration of 10 ms [13]. Based on this data, one can calculate the characteristic length within the water that is effectively accelerated before the explosion pressure is relieved at the water-air surface. In this case the propagation length is 1–7 m depending on the two-phase sound speed in water above the stratified melt. This estimate suggests that the wave generated by the impulse will propagate rapidly and it will be relieved when the wave reaches free surface in 10 ms. Thus, it is hard to define the exact accelerated water mass as limited to just the melt spreading diameter. Assuming m_{w} as the total water mass in the test chamber provides a reasonable bound for the reported efficiency calculation. If one uses the total water mass for the calculation, steam explosion efficiency will be a factor of 20 times lower that the reported efficiencies calculated for a 0.4 m diameter x 0.16 m height water column at PULiMS and a factor of 10 times lower for the SES tests (Fig. 1).

2.3. Discussion of the melt intermixing depth

Considering that the amount of the molten liquids participating in the energy transfer is also a key to the energetics of the explosion, the depth of intermixing is an important parameter to estimate in a stratified steam explosion. Bang and Corradini [8] investigated experimentally the fuel-coolant intermixing depth with a well-defined initial geometry for simulant fuel-coolant pairs. In these experiments, they varied the initial depth of the bottom hot liquid layer. This method is based on the hypothesis that the mechanical work output in a stratified vapor explosion does not change until the initial depth of the hot bottom liquid layer is reduced to near the depth of intermixing and that mechanical work would decrease as the depth is reduced further. The effect of the overlying liquid volume was investigated by varying this liquid layer depth. They reported that the mechanical work output increased as the depth of overlying liquid increased within the range of the available volume in the experiments. They developed a mechanistic model (based on the role of Ralyeigh-Taylor instabilities and film boiling collapse) that predicts an intermixing depth for entire explosion period equal to:

$$L_{mix} = \left[\left(\frac{4}{27}\right)\left(\frac{1}{a\sigma}\right)\frac{(\rho_l-\rho_v)^3}{(\rho_l+\rho_v)^2}\right]^{-1/4}\left[1+\left(\frac{\rho_l'}{\rho_l}\right)^{1/2}\right]^{-1}\left(\frac{d}{c}\right) \quad (3)$$

where a is the magnitude of acceleration due to film collapse, ρ_l, ρ_v and ρ_l' are density of top liquid, top vapor, and bottom liquid, respectively, c denotes the sonic speed in the top liquid layer and d indicates the depth of the top liquid layer. Note the linear relationship between the depth of the top liquid layer and the depth of penetration. This relationship was verified for small liquid layer depths, but could be unrealistically large if the top liquid layer is sufficiently deep. In such a case, however, the jet penetration time would be limited by other factors such as boiling and jet breakup. It is expected that the work output will reach a plateau for pool depths larger than a few tens of centimeters, but these large depths were not investigated in these previous experiments.

This relationship between the proposed intermixing length with the depth of overlying liquid is considered to be an upper bound. Therefore, one could use this approach to bound the stratified steam explosion energetics for severe accident conditions. This is the approach taken in Section 3 of this report.

3. Limits to stratified steam explosion energetics as compared to pouring contact mode

In this section, we calculate the limits on explosion energetics based on our theoretical models that predict fuel-coolant mixing mechanisms for a stratified steam explosion compared to a steam explosion in pool geometry. This approach presents a general bounding analysis that includes different mixing phenomena in different steam explosion configurations. For a stratified geometry, we employ Bang's model for fuel mixing-fragmentation mechanism [8] to estimate the amount of fuel mass involved in an explosion compared to the fuel explosion mass involved based on our model for fuel fragmentation for a pool geometry [15].

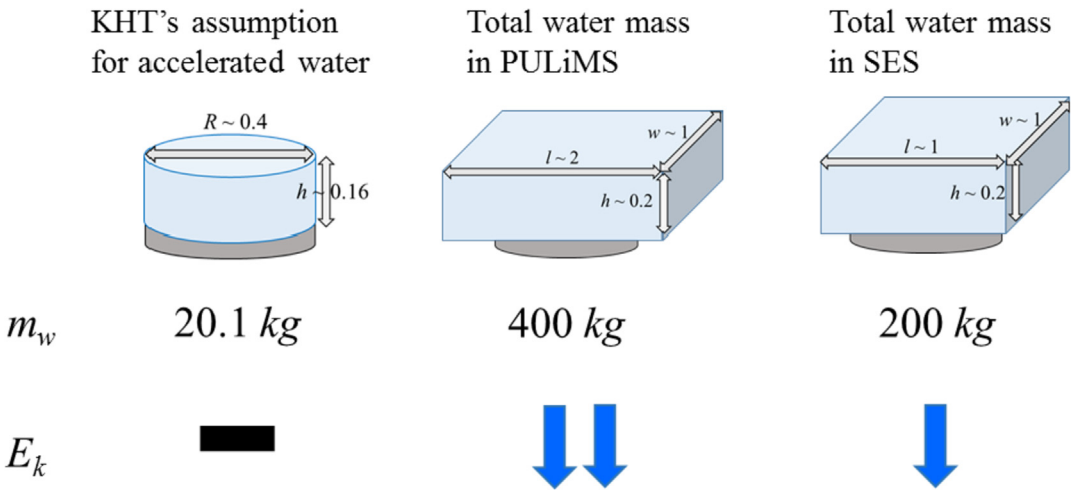

Fig. 1. Schematics of the mass of accelerated water (the black bar is the assumed slug mass by KTH, while the actual slug mass is larger and bounded and this larger water mass would imply a notable decrease the reported kinetic energy).

3.1. Review of the fuel mixing-fragmentation mechanism of the stratified steam explosion

In a stratified vapor explosion in which the two liquid layers initially are completely separated by a vapor film, vapor film collapse on the arrival of the propagating explosion front causes pressure driven interpenetration of the two liquids that results in the rapid energy transfer and vaporization of the cold liquid. Then, the high-pressure vapor region expands, working against the surroundings. The rapid liquid-liquid mixing behind this shock front may involve a number of mixing phenomena: i.e., Rayleigh-Taylor (RT) instability, Kelvin-Helmholtz (KH) instability and convective turbulent mixing. Based on Bang et al. [8], the RT instability is the primarily mechanism. The explosion front pressure propagates faster through the liquid phase along the stratified interface causing the vapor film to begin to collapse. The vapor film pressure increases and then the acceleration of the interface is now directed from the vapor to the liquid, causing RT instabilities to occur. This causes jets of the overlying liquid to penetrate into the other liquid (Fig. 2).

In this stratified geometry, the magnitude of the acceleration is given [8] by

$$a = (P_v - P_\infty)/\rho_l L_c \tag{4}$$

where L_c is the curvature of the liquid-vapor interface. An appropriate choice for the length scale, L_c, is the Taylor wavelength under the gravitational acceleration.

$$L_c \sim 2\pi\left[\sigma/g(\rho_l - \rho_v)\right]^{1/2} \tag{5}$$

The initial jet velocity can be approximated to be the product of the acceleration and an acceleration time scale as $v_{jet} = a\tau$. For the acceleration time (τ), the characteristic time scale of the instability wave growth, corresponding to the fastest growing wavelength, is given by

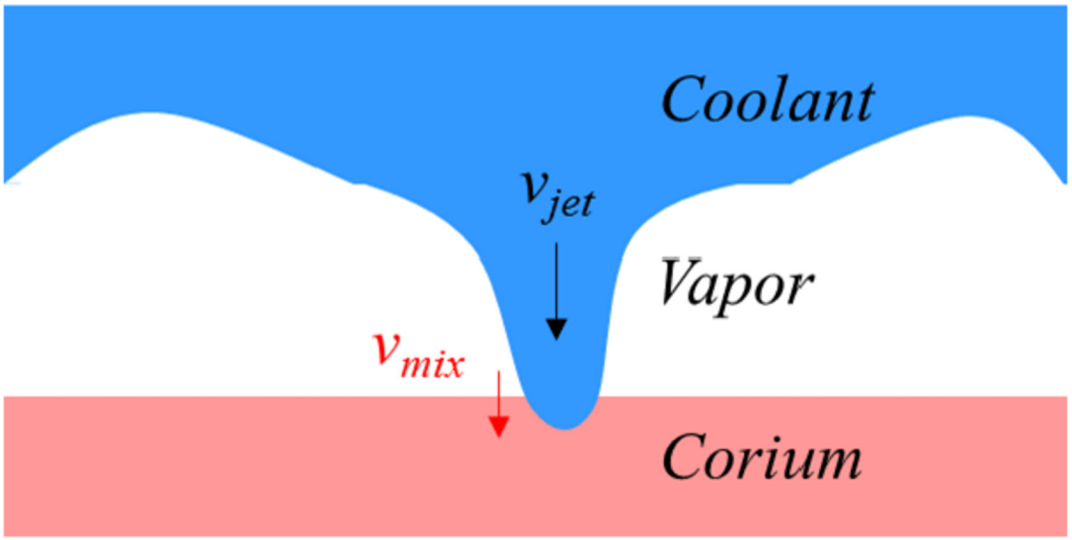

Fig. 2. Schematic of the explosive mixing mechanism in a stratified geometry.

$$\tau = \left[\frac{4}{27}\frac{a^3(\rho_l-\rho_v)^3}{\sigma(\rho_l+\rho_v)^2}\right]^{-1/4} \tag{6}$$

Using Eqs. (4)–(6), one can obtain the initial jet velocity;

$$v_{jet} = a\tau = a\left[\frac{4}{27}\frac{a^3(\rho_l-\rho_v)^3}{\sigma(\rho_l+\rho_v)^2}\right]^{-1/4} = \left[\frac{27}{4}\frac{\sigma(\rho_l+\rho_v)^2}{a(\rho_l-\rho_v)^3}\right]^{1/4}$$
$$= \left[\frac{27}{4}\frac{\rho_l L_c}{(P_v-P_\infty)}\frac{\sigma(\rho_l+\rho_v)^2}{(\rho_l-\rho_v)^3}\right]^{1/4} \tag{7}$$

Since the liquid density is much higher than vapor density, Eq. (7) can be simplified as

$$v_{jet} = \left[\frac{27}{4}\frac{L_c\sigma}{(P_v-P_\infty)}\right]^{1/4} = \left[\frac{27\pi}{2}\left(\frac{\sigma}{g\rho_l}\right)^{1/2}\frac{\sigma}{(P_v-P_\infty)}\right]^{1/4} \tag{8}$$

The initial jet penetration velocity v_{mix} on contact with the bottom liquid (stratified fuel) can be obtained from the steady-state Bernoulli's equation for inviscid flow. Considering the pressure equilibration at the stagnation point, one obtains

$$\frac{1}{2}\rho_l(v_{jet}-v_{mix})^2 + P = \frac{1}{2}\rho_l' v_{mix}^2 + P \rightarrow v_{mix} = v_{jet}\Big/\left[1+\left(\frac{\rho_l'}{\rho_l}\right)^{1/2}\right] \tag{9}$$

where prime ' denotes the bottom liquid. Thus, v_{mix} indicates the penetration rate into stratified fuel.

In this discussion, we have conservatively assumed that whole stratified fuel-coolant interface will be involved in an explosion simultaneously. This cannot happen in reality as the propagation time is not instantaneous, but this assumed planar source for the total fuel mass involved in the explosion provides an upper bound energetics value for the stratified explosion. So, the surface area of stratified fuel, A_{str}, exposed to this explosive mixing is defined by the geometry of stratified pool with a square cavity of width, w ($A_{str} = w^2$). The mixing rate in a stratified geometry in a square cavity can be expressed as

$$\dot{m}_{mix} \sim \rho_f \dot{V}_{str} = \rho_f w^2 v_{mix}$$
$$= \rho_f w^2\left[\frac{27\pi}{2}\left(\frac{\sigma}{g\rho_l}\right)^{1/2}\frac{\sigma}{(P_v-P_\infty)}\right]^{1/4}\left[1+\left(\frac{\rho_l'}{\rho_l}\right)^{1/2}\right]^{-1} \tag{10}$$

3.2. Review of the fuel fragmentation mechanism for the pouring mode steam explosion

In a pool geometry, Kim's fragmentation model [16] assumes that rapid fuel fragmentation is caused by a combination of hydrodynamic and thermal effects. The process of rapid fuel particle fragmentation is described as occurring in four steps: (1) Film boiling around molten fuel particles in the coolant liquid; (2) Unstable wave development at the coolant vapor-liquid interface caused by the external pressure pulse, which initiates film collapse, and subsequent coolant jet formation due to RT instabilities in a spherical geometry; (3) Jet impingement on and likely penetration of the molten fuel surface, and coolant encapsulation within the fuel; and (4) Expansion of the molten fuel surface due to rapid evaporation of the encapsulated coolant and fragmentation of the fuel into smaller fragments that quench. In this work, a semi-empirical model proposed by Tang et al. [15] is used to describe this fuel fragmentation process and rate of fuel breakup. Given the four-step conceptual picture described above, the fragmentation rate is proportional to the corium droplet surface area and the average jet velocity during the process;

$$\dot{m}_f \sim \rho_c \dot{V}_{pool} \sim \rho_f \pi D_{mix}^2 N_p v_{jet} F(\alpha) g(\tau) \tag{11}$$

where D_{mix} is the fuel particle diameter resulting from initial fuel jet mixing in the coolant pool; N_p is the number of particles at that mixing diameter; v_{jet} is the coolant jet velocity, $F(\alpha)$ is the suppression factor for large coolant void fraction; $g(\tau)$ is the factor for the available fragmentation time (Fig. 3).

Knowing the melt-jet diameter ($D_{m\text{-}jet}$) and coolant pool height (H), the fuel particle number N_p can be estimated as

$$N_p = \frac{\pi D_{m-jet}^2 H}{\frac{\pi}{6}D_{mix}^3} \tag{12}$$

Eq. (12) provides the maximum number of fragmented particles, which describes the largest explosion energetics in pouring-mode pool configuration for the bounding analysis conducted in this study. The jet velocity v_{jet} is approximated based on the growth rate of coolant disturbances on the fuel particle surfaces. In the process of fuel particle fragmentation, the stages of vaporization of the entrapped coolant and the accompanying fuel fragmentation occur on a much smaller time scale than the stages of coolant jet formation and jet penetration into the fuel. The process of coolant jet entrapment consists of three steps: vapor film collapse, jet formation, and jet penetration. The first two processes occur simultaneously and determine the velocity of the jet entering the fuel. The jet velocity is in turn determined by the growth rate of surface disturbances on the fuel. In Kim's analysis [16], this rate was calculated based on RT instability. Therefore we have:

$$v_{jet,f} \sim C\cdot(a\,\lambda)^{0.5} \tag{13}$$

where C is constant, λ is the wavelength, which is proportional to the fuel drop's radius $D_{mix}/2$, and a is the acceleration caused by the rise of local pressure of the vapor. From Rayleigh's equation for a spherical geometry, a can be approximated for the initial jetting behavior as [17]:

$$a = \frac{2(P-P_{th})}{\rho_l D_{mix}} \tag{14}$$

where P is the local explosion pressure, and P_{th} is the threshold pressure for film collapse. According to the theoretical work of Kim [16], and the experimental results of Nelson [18], the threshold pressure is in the range of a few bars; i.e., nearly ambient pressure. As the ambient pressure rises, the threshold pressure also rises [18]; however, no definite quantitative values have been suggested from the data. In our model, the threshold pressure of 0.2 MPa has been chosen for the ambient pressure condition.

The factor $F(\alpha)$ is introduced to keep this correlation consistent with the mechanisms of the model because film collapse and coolant jet impingement gradually become less likely to occur as the vapor fraction increases. The factor F decreases from 1 to 0 at $\alpha = 50\%$, corresponding to reasonable transition from the bubbly flow to the droplet flow regime. The factor $g(\tau)$ is introduced into

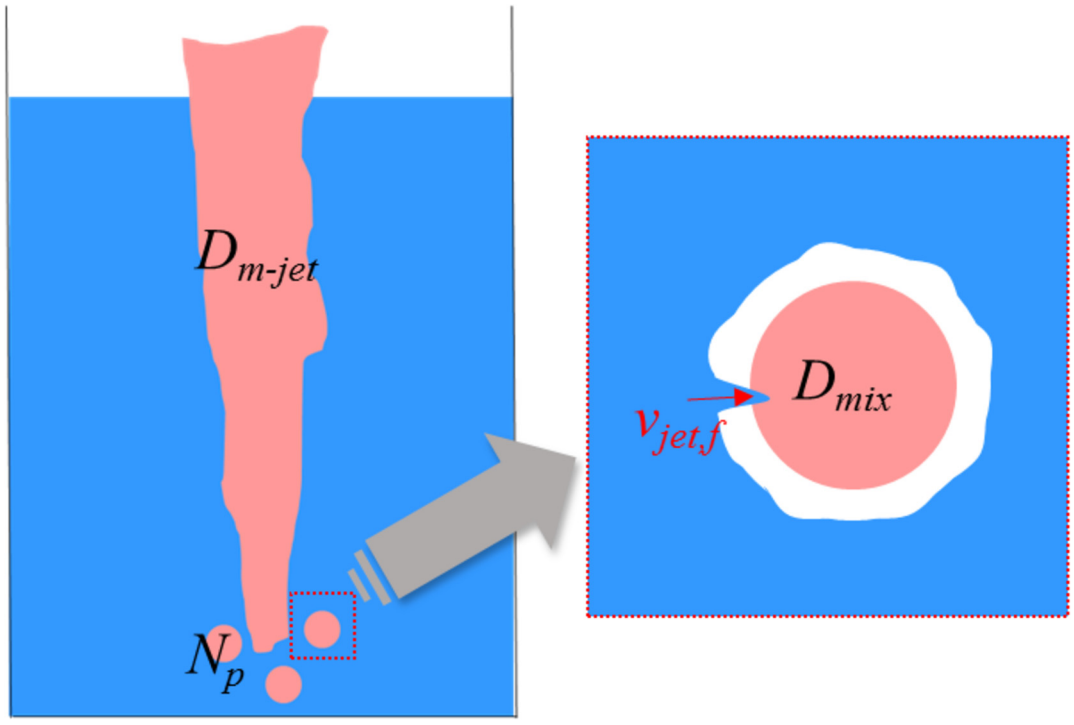

Fig. 3. Schematic of the fragmentation mechanism in a pool geometry.

the model as our empirical approach to account for the characteristic time, τ, available for this fragmentation mechanism to be operative before depressurization occurs from the coolant pool surface. In this analysis, the factors $F(\alpha)$ and $g(\tau)$ are assumed to be unity '1' because we are focusing on initial steam explosion stage.

Substituting Eqs. (12), (13), and (14) into Eq. (11), we get the final expression for the rapid fuel fragmentation rate as a function of the local variables in the fuel coolant mixture:

$$\dot{m}_f \sim \rho_f \dot{V}_{pool} \sim C\rho_f \pi \frac{6D_{m-jet}^2 H}{D_{mix}} \left(\frac{(P-P_{th})}{\rho_c}\right)^{0.5} \tag{15}$$

The constant, C, in this discussion is chosen as 0.01 based on Tang's original analysis [15] in which this constant value, C, is found to empirically bound the experimental data from KROTOS experiments [19]. It is recognized that this approach to the analysis is not completely mechanistic, but semi-empirical based on the prototypic KROTOS test data.

3.3. Comparison of fuel masses involved in a steam explosion for a stratified and pool geometry

From Eqs. (10) and (15), we can calculate how much fuel would rapidly fragmented and drive the energetics of the steam explosion for a stratified and pool configuration respectively. So, by comparing these fuel fragmentation masses involved for a stratified steam explosion, $\dot{m}_{str}$, and for a pool steam explosion, $\dot{m}_{pool}$, we can predict which geometry would produce the more energetic steam explosion. When this ratio of masses for stratified to pool steam explosions is larger than '1', it indicates that a steam explosion in a stratified geometry would be more energetic than for one in a pool geometry.

$$\frac{\dot{m}_{str}}{\dot{m}_{pool}} = \frac{\dot{m}_{mix}}{\dot{m}_f} = \frac{w^2 \left[\frac{27\pi}{2}\left(\frac{\sigma}{g\rho_l}\right)^{1/2} \frac{\sigma}{(P_v - P_\infty)}\right]^{1/4} \left[1 + \left(\frac{\rho_l'}{\rho_l}\right)^{1/2}\right]^{-1}}{C\pi \frac{6D_{m-jet}^2 H}{D_{mix}} \left(\frac{(P-P_{th})}{\rho_c}\right)^{0.5}} \tag{16}$$

For a quantitative comparison, we use a cavity geometry, explosion pressure, and fuel mixing diameter in a prototypic range, along with water properties. Table 1 shows all reference values used in this comparison. From these values, we vary key parameters individually, except water properties, to show the parameter effect. In these comparisons, the water pool depth, H, is used as a main parameter since it is believed that H could describe the geometric transition from pool to stratified configuration. The density of fuel is assumed to be 8000 kg/m^3 for prototypic conditions, but it also varied based on densities of simulant materials. The densities of simulant materials are 8900 kg/m^3 for Bi_2O_3, 7160 kg/m^3 for WO_3, and 5890 kg/m^3 for ZrO_2; i.e., KTH used eutectic materials composed of Bi_2O_3, WO_3, and ZrO_2 [14].

In this study, with varied parameters and H in proper range, we calculate the critical condition for $D_{\text{m-jet}}$, $D_{\text{m-jet, c}}$, having same fuel masses involved in an FCI for a stratified and pool geometry steam explosion (when the ratio of masses for stratified to pool steam explosions [Eq. (16)] is '1').

Table 1
Summary of parameters used in this calculation.

Parameter	Value
D_{mix}	1 cm
$\Delta P \sim (P - P_{th})$	10 MPa
$\Delta \rho \sim (\rho_l - \rho_v)$ for water	1000 kg/m^3
ρ'	8000 kg/m^3
σ for water	0.05 N/m
w	5 m

$$w^2\left[\frac{27\pi}{2}\left(\frac{\sigma}{g\rho_l}\right)^{1/2}\frac{\sigma}{(P_v-P_\infty)}\right]^{1/4}\left[1+\left(\frac{\rho_l'}{\rho_l}\right)^{1/2}\right]^{-1} = C\pi\frac{6D_{m-jet,\,c}^2 H}{D_{mix}}\left(\frac{(P-P_{th})}{\rho_c}\right)^{0.5} \rightarrow D_{m-jet,\,c}$$
$$= \sqrt{w^2\left[\frac{27\pi}{2}\left(\frac{\sigma}{g\rho_l}\right)^{1/2}\frac{\sigma}{(P_v-P_\infty)}\right]^{1/4}\left[1+\left(\frac{\rho_l'}{\rho_l}\right)^{1/2}\right]^{-1}\left\{C\frac{6\pi H}{D_{mix}}\left(\frac{(P-P_{th})}{\rho_l}\right)^{0.5}\right\}^{-1}} \quad (17)$$

It indicates that, if melt jet is smaller than $D_{m\text{-}jet,\,c}$, a stratified geometry will be more energetic with more fuel mass involved in a steam explosion otherwise a pool geometry will be dominant with larger steam explosion energetics (see Fig. 4).

Figs. 4–7 shows that the effects of H, D_{mix}, w, ρ' and ΔP on $D_{m\text{-}jet,\,c}$. H and D_{mix} are the parameters related with pool configuration steam explosion. Increasing D_{mix} under given $D_{m\text{-}jet}$ will decrease the interfacial area of fragmented particles in pool configuration, thereby resulting in less mass rate participating to steam explosion in a pool geometry. But a larger H will lead to the opposite result by increasing interfacial area. Cavity dimension w and fuel density ρ' are associated with stratified steam explosion configuration. A larger cavity dimension, w, could provide more surface area for the stratified steam explosion. The fuel density ρ' affects the initial jet penetration velocity v_{mix}. A larger fuel density reduces the jet penetration on the fuel side, therefore it will have a smaller mass involved for stratified steam explosion. We would note that the penetration velocity of fuel in Bang's model [8] was theoretically calculated from the jet velocity of water using Bernoulli's equation, while Tang [15] used the empirical constant C to get the penetration velocity from water jet velocity based on experimental results.

The generated pressure ΔP is an important parameter in both geometries, but the effect is more significant in a pool geometry (Fig. 7). It is attributed to the difference in the wavelength associated with RT instability for different geometries. While this instability is primarily considered in both analyses, the wavelength for a stratified geometry compared to a pool geometry are defined differently. In a stratified geometry Taylor wavelength under the gravitational acceleration is a reasonable choice, since we have a planar geometry. In contrast the fragmented particle radius is used in a pool geometry due to a spherical geometry of the fuel particle. Consequently, increasing ΔP induces more energetic steam explosion for pool configuration.

To summarize, using Eq. (17), one can compare the fuel mass involved in a steam explosion in a stratified geometry compared to the fuel mass involved in a pool geometry. As shown in Fig. 4, there

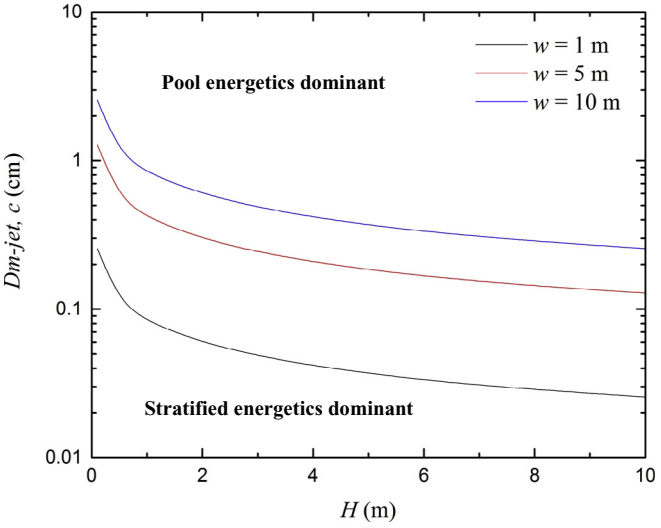

Fig. 5. $D_{m\text{-}jet,c}$ as a function of H with varying width of the cavity (w).

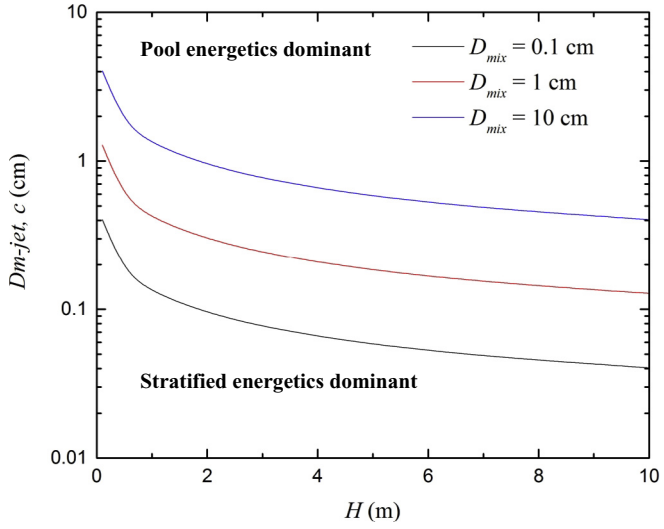

Fig. 4. $D_{m\text{-}jet,c}$ as a function of H with varying mixing diameter (D_{mix}).

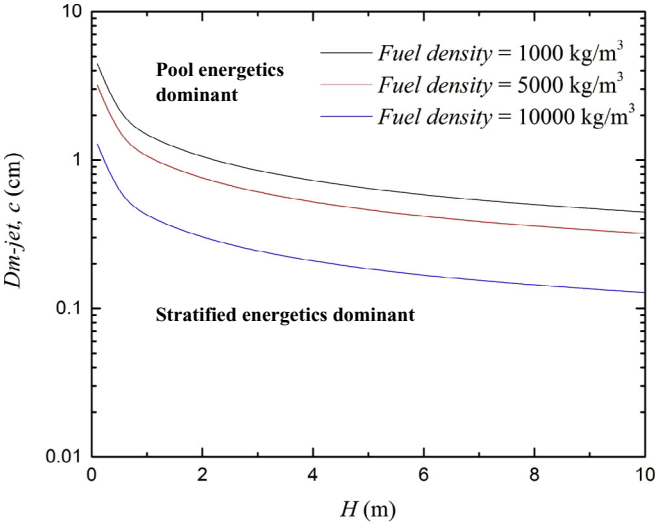

Fig. 6. $D_{m\text{-}jet,c}$ as a function of H with varying fuel density (ρ')

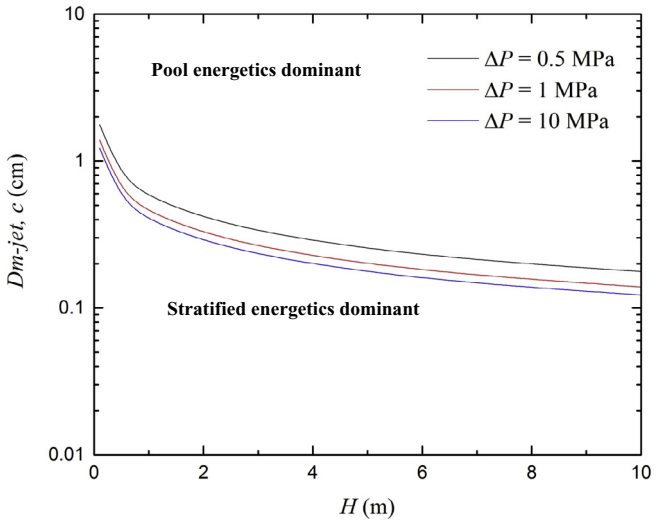

Fig. 7. $D_{m\text{-}jet,c}$ as a function of H with varying generated pressure (ΔP).

is a limited set of conditions under which a steam explosion is more energetic in a stratified geometry. In particular when melt jet diameter is small, the stratified configuration explosion could produce larger steam explosion energetics than the pouring mode. While the stratified explosion would be more energetic on a relative basis the absolute energetic explosion output would be small, since the total fuel mass involved would still be quite small.

4. Discussion and conclusion

In this work, we have examined the current state of knowledge for stratified steam explosions by examining followed general areas:

- A review of previous stratified steam explosion experiments including recent KTH's work,
- Established fuel-coolant limits on explosion energetics based on corresponding fuel mixing mechanisms for stratified steam explosion compared to fuel mixing in a pool geometry.

Some previous experiments reported stratified steam explosions, but the detailed conditions for the explosion have not been revealed to date. Based on our review, the explosion energetics in a stratified geometry appears weaker. For a more in-depth discussion, we developed a theoretical approach to compare the energetics for stratified-mode and pouring-mode steam explosions energetics. This evaluates how much molten fuel would participate steam explosion for different configurations, and then compare the fuel mass involved in a steam explosion in a stratified geometry compared to pool geometry. Consequently, we can suggest a limited set of conditions under which a steam explosion is more energetic for a stratified geometry. We find that when melt jet diameter is small (~1 cm), the stratified configuration explosion could produce larger steam explosion energetics. While the stratified explosion would be more energetic on a relative basis the absolute energetic explosion output would be small as the calculation indicates. This is the case, since the total fuel mass involved would still be quite small. Therefore, we conclude that the likelihood is quite small to have more energetic steam explosion in a stratified geometry compared to a typical pool geometry that would present a challenge to containment integrity.

Conflicts of interest

The authors declare that they have no conflict of interests.

Acknowledgement

This study is supported by U.S.NRC(United States Nuclear Regulatory Commission).

Nomenclature

Roman symbols

a	Magnitude of acceleration by film collapse
A	Area
c	Sonic speed
d	Depth of the top liquid layer for stratified configuration
D_{mix}	Fuel particle diameter from initial fuel jet mixing
$D_{m\text{-}jet}$	Melt-jet diameter
E	Energy
g	gravity acceleration
H	Pool height
I	Impulse
L_c	Curvature of liquid-vapor interface
L_{mix}	Intermixing depth
m_w	Mass of accelerated water
$\dot{m}_{mix}$	Mixing mass rate for stratified configuration
$\dot{m}_f$	Fragmentation rate for pool configuration
N_p	Number of particles
P	Pressure
P_{th}	Threshold pressure
v_{jet}	Jet velocity
v_{mix}	Initial jet penetration velocity
$\dot{V}$	Mixing volume rate
w	Width of cavity

Greek symbols

α	Vodifraction
ε	Steam explosion efficiency
ρ	Density
ρ'	Molten fuel (or bottom material for stratified configuration) density
σ	Surface tension
τ	Acceleration time
λ	Wavelength

Subscript

l	Liquid
v	Vapor
∞	Bulk
str	Stratified configuration
pool	Pool configuration
released	Released energy
t	Thermal energy
k	Kinetic energy

References

[1] M.L. Corradini, B.J. Kim, M.D. Oh, Vapor explosions in light water reactors: a review of theory and modeling, Prog. Nucl. Energy 22 (1988) 1–117.
[2] D.F. Fletcher, R.P. Anderson, A review of pressure-induced propagation models of the vapour explosion process, Prog. Nucl. Energy 23 (1990) 137–179.
[3] M.L. Corradini, R.P. Taleyarkhan, Vapor explosions: a review of experiments for accident analysis, Nucl. Saf. 32 (1991).
[4] D.F. Fletcher, A review of the available information on the triggering stage of a steam explosion, Nucl. Saf. 35 (1994).

[5] T.G. Theofanous, M. Saito, An assessment of Class-9 (core-melt) accidents for PWR dry-containment systems, Nucl. Eng. Des. 66 (1981) 301–332.
[6] M. Pilch, Acceleration Induced Fragmentation of Liquid Drops, 1982.
[7] C.C. Chu, M.L. Corradini, One-dimensional transient fluid model for fuel/coolant interaction analysis, Nucl. Sci. Eng. 101 (1989) 48–71.
[8] K.H. Bang, M.L. Corradini, Vapor explosions in a stratified geometry, Nucl. Sci. Eng. 108 (1991) 88–108.
[9] M. Berman, Light Water Reactor Safety Research Program Quarterly and Semiannual Report, October 1983-March 1984, NUREG/CR-4459, SAND-85–2500, Sandia National Laboratory, 1986.
[10] R. Silverii, D. Magallon, FARO LWR Programme–test L-31 Data Report, Technical Note, European Commission Joint Research Centre ISPRA, 1999. No. I. 99.
[11] R. Anderson, D. Armstrong, D. Cho, A. Kras, Experimental and Analytical Study of Vapor Explosions in Stratified Geometries, Argonne National Lab, IL (USA), 1988.
[12] A. Konovalenko, A. Karbojian, P. Kudinov, Experimental results on pouring and underwater liquid melt spreading and energetic melt-coolant interaction, in: The 9th International Topical Meeting on Nuclear Thermal-Hydraulics, Operation and Safety (NUTHOS-9), Kaohsiung, Taiwan, September 9–13, American Nuclear Society, 2012.
[13] D. Grishchenko, A. Konovalenko, A. Karbojian, V. Kudinova, S. Bechta, P. Kudinov, Insight into steam explosion in stratified melt-coolant configuration, in: 15th International Topical Meeting on Nuclear Reactor Thermal Hydraulics, NURETH-15, 12 to 17 May, 2013, Pisa, Italy, 2013.
[14] P. Kudinov, D. Grishchenko, A. Konovalenko, A. Karbojian, S. Bechta, Investigation of steam explosion in stratified melt-coolant configuration, in: The 10th International Topical Meeting on Nuclear Thermal-Hydraulics, Operation and Safety (NUTHOS-10), 2014, pp. 14–18.
[15] J. Tang, M.L. Corradini, Modelling of the Complete Process of One-dimensional Vapor Explosions, 1994.
[16] B.-J. Kim, Heat Transfer and Fluid Flow Aspects of a Small Scale Single Droplet Fuel-coolant Interaction, Wisconsin Univ., Madison (USA), 1985.
[17] M.D. Oh, M.L. Corradini, A propagation/expansion model for large scale vapor explosions, Nucl. Sci. Eng. 95 (1987) 225–240.
[18] L.S. Nelson, P.M. Duda, Steam Explosion Experiments with Single Drops of Iron Oxide Melted with a CO/sub 2/laser. Part II. Parametric Studies, Sandia National Labs, Albuquerque, NM (USA), 1985.
[19] R.H. Chen, M.L. Corradini, G.H. Su, S.Z. Qiu, Analysis of KROTOS steam explosion experiments using the improved fuel-coolant–interaction code Texas-VI, Nucl. Sci. Eng. 174 (2013) 46–59.